Energy Environ Sci. 2021 Mai 19; 14(5): 2520–2534.
Online veröffentlicht am 2021. März 31. doi: 10.1039/d0ee03763j
PMCID: PMC8133363
PMID: 34046082

Vom Birkeland-Eyde-Verfahren zum energieeffizienten plasmabasierten NO_X Synthese: Eine techno-ökonomische Analyse

Kevin H. R. Rouwenhorst, Fatme Jardali, Annemie Bogaerts, und Leon Lefferts

Abstrakt

Plasmabasiertes NO_X Synthese *über* das Birkeland-Eyde-Verfahren war eine der ersten industriellen Fixierungsmethoden. Diese Technologie spielte jedoch nie eine dominierende Rolle für die Stickstofffixierung aufgrund der Erfindung des Haber-Bosch-Verfahrens. In jüngster Zeit hat die Stickstofffixierung durch Plasmatechnologie deutlich an Bedeutung gewonnen aufgrund des Aufkommens von kostengünstigem, erneuerbarem Strom. Wir präsentieren zunächst einen kurzen historischen Hintergrund von plasmabasiertem NO_X Synthese. Danach diskutieren wir die berichtete Leistung für plasmabasiertes NO_X Synthese in verschiedenen Arten von Plasmareaktoren, zusammen mit der Verständnis der Reaktionsmechanismen in der Plasmaphase, sowie auf einer katalytischen Oberfläche. Abschließend vergleichen wir die plasmabasierten $NEIN_X$ Syntheseprozess mit dem auf Elektrolyse basierenden Haber-Bosch-Verfahren in Kombination mit dem Ostwald-Verfahren in Bezug auf die Investitionskosten und Energieverbrauch. Diese Analyse zeigt, dass die Energieverbrauch für NO_X Die Synthese mit Plasmatechnologie ist mit dem derzeit besten Wert von 2,4 MJ mol N nahezu konkurrenzfähig mit dem kommerziellen Verfahren^{-1}, die weiter auf etwa 0,7 MJ mol N absinken muss^{-1} um voll wettbewerbsfähig zu werden. Dies kann erreicht werden durch: Weitere Optimierung des Plasmareaktors und effektiver Plasma-Katalysator Kupplung.

Plasmabasiertes NO_X Synthese kann mit erneuerbarem Strom für dekarbonisierte Herstellung von Düngemitteln. Erneutes Forschungsinteresse führt dazu, dass wettbewerbsfähig mit dem herkömmlichen Verfahren.

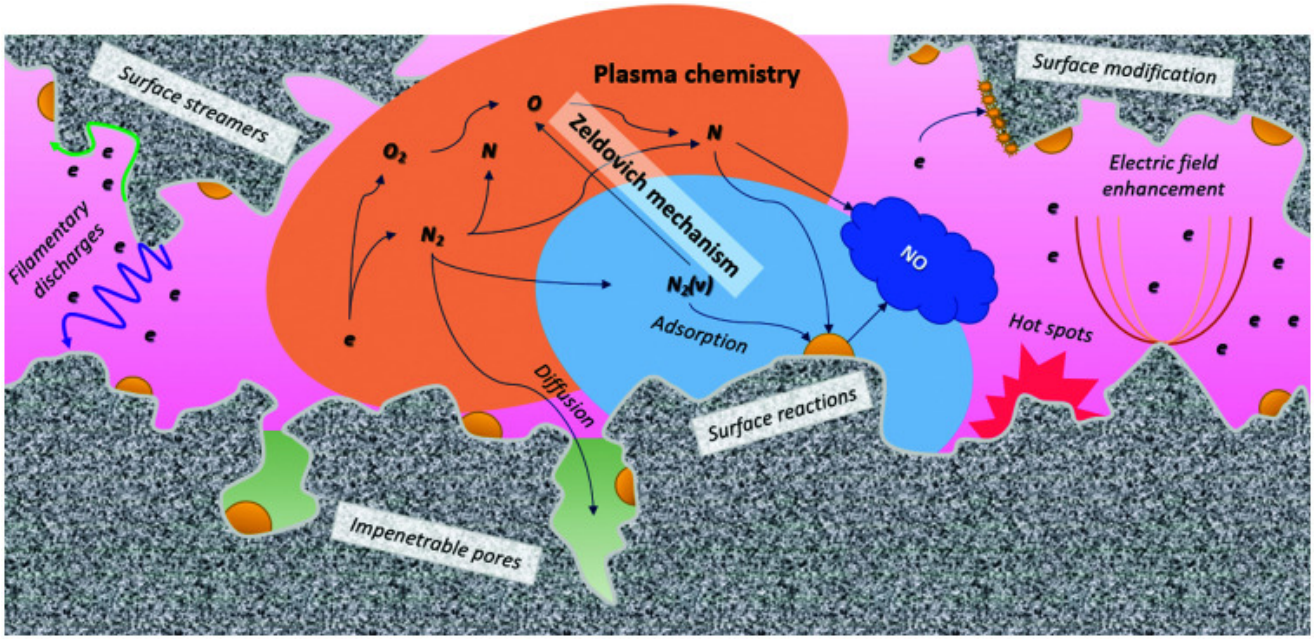

Breiterer Kontext

Industriell Die Stickstofffixierung wurde zunächst als plasmabasierte Birkeland-Eyde-Prozess vor etwa einem Jahrhundert, obwohl dieser Prozess schließlich vom Haber-Bosch-Verfahren aufgrund der geringeren Energieverbrauch für die Stickstofffixierung des Haber-Bosch-Verfahrens. Die Stickstofffixierung ist derzeit stark zentralisiert, da die Temperatur- und Hochdrucksynthese von Ammoniak *über* die Haber-Bosch-Verfahren. Aufgrund des Aufkommens kostengünstiger erneuerbarer Energien Strom aus Sonne und Wind gibt es ein erneutes Interesse an Dezentrale Möglichkeiten der strombetriebenen Stickstofffixierung. In In den letzten Jahren haben computergestützte Studien die Verständnis der plasmabasierten Stickstofffixierung. Dies hat es ermöglicht, optimierte Plasmareaktoren mit reduziertem Energieverbrauch für plasmabasiertes NO_X Synthese. Dies hat zu einer erneuten Interesse am plasmabasierten Stickstofffixierungsverfahren für dezentrale und bedarfsgerechte Düngemittelproduktion. Die jüngste Entwicklungen werden im aktuellen Analysepapier diskutiert, ebenso wie Energieverbrauchsziele für die erneute Kommerzialisierung plasmabasierter Stickstofffixierung.

Introduction

For over a century, nitrogen (N_2) has been industrially fixed into reactive nitrogen (N_r) compounds to increase agricultural yields.[1] In order to artificially fix atmospheric N_2, different attempts have been made throughout the years, including the Birkeland–Eyde (B–E) process that produces NO_X,[2] the Frank–Caro (F–C) process that produces calcium cyanamide,[3] and the Haber–Bosch (H–B) process that produces ammonia (NH_3),[4] among others. Nowadays, nitrogen is almost exclusively fixed *via* the Haber–Bosch process.[4] An overview of the annual consumption of fixed nitrogen from various natural sources and from industrial nitrogen fixation

technologies is shown in Fig. 1. Guano and Chile saltpetre are natural sources of fixed nitrogen, mostly derived from Chile and Peru.[4] Ammonium sulphate is a by-product of coke ovens and of caprolactam production.

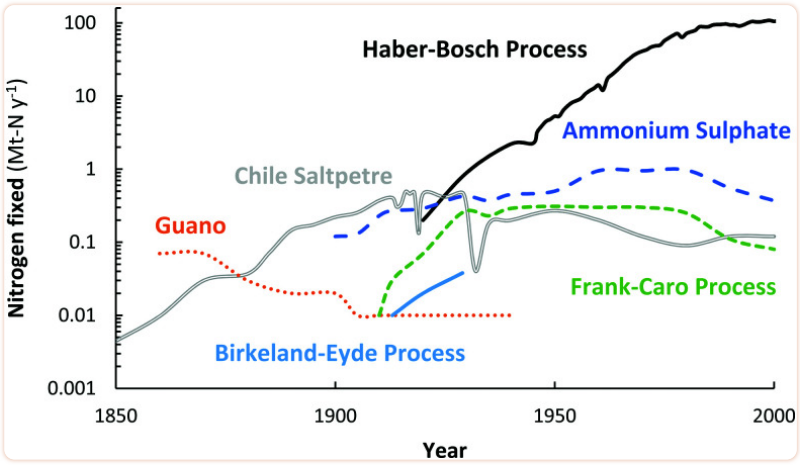

Fig. 1

Annual consumption of fixed nitrogen from various natural sources and from industrial nitrogen fixation technologies. Original sources.[2,4,5]

In 1903, the first synthetic plasma-based NO_X synthesis process was developed and tested in Christiania University (nowadays known as the University of Oslo) by Kristian Birkeland and Samuel Eyde. In the B–E process, air was passed through an electric arc, *i.e.*, a thermal plasma, thereby producing nitrogen oxide (NO) and nitrogen dioxide (NO_2) (eqn (1) and (2)). Thereafter, NO_2 was concentrated and absorbed in water to form nitric acid (HNO_3) (eqn (3)).

Nitric acid can also be produced *via* the combined Haber–Bosch (H–B) and Ostwald process. In the H–B process, ammonia (NH_3) is synthesized from hydrogen (H_2) and atmospheric nitrogen (N_2) (eqn (4)). The NH_3 produced by the H–B process is then oxidized in the Ostwald process to form NO and NO_2 (eqn (2) and (5)). Subsequently, the NO_2 is absorbed in water to from HNO_3. In both processes, the resulting product is HNO_3, which can be neutralized with NH_3 to form ammonium nitrate (NH_4NO_3) (eqn (6)). NH_4NO_3 is primarily used as a fertilizer for agricultural activity and as an explosive for the mining industry. NH_4NO_3 production accounts for about 75–80% of the HNO_3 produced.[6] Further uses of HNO_3 include nitration reactions, its usage as oxidant and as rocket propellant.

$$N_2 + O_2 \rightleftharpoons 2NO.\ \text{with}\ \Delta H^{o}_{r} = 180\ \text{kJ mol}^{-1}. \quad (1)$$

$$2NO + O_2 \rightarrow 2NO_2.\ \text{with}\ \Delta H^{o}_{r} = -114\ \text{kJ mol}^{-1}. \quad (2)$$

$$3NO_2 + H_2O \rightarrow 2HNO_3 + NO.\ \text{with}\ \Delta H^{o}_{r} = -117\ \text{kJ mol}^{-1}. \quad (3)$$

$$3H_2 + N_2 \rightarrow 2NH_3.\ \text{with}\ \Delta H^{o}_{r} = -92\ \text{kJ mol}^{-1}. \quad (4)$$

$$4NH_3 + 5O_2 \rightarrow 4NO + 6H_2O.\ \text{with}\ \Delta H^o_r = -905\ \text{kJ mol}^{-1}. \quad (5)$$

$$NH_3 + HNO_3 \rightarrow NH_4NO_3. \quad (6)$$

Throughout the years, different factors played a role in the abandonment of the plasma-based B–E process in favour of the fossil-fuel powered H–B technology, including (i) emergence of low-cost fossil fuels such as coal and natural gas, (ii) the substantially lower energy cost for nitrogen fixation *via* the thermochemical H–B process (about 0.5–0.6 MJ mol N^{-1}) as compared to the plasma-based B–E process (about 2.4–3.1 MJ mol N^{-1}),[7–10] (iii) the higher capital investment for the B–E compared to the combined H–B and Ostwald process,[2] and (iv) the higher maintenance cost of the B–E reactor.[2,11] Therefore, NO_X production *via* NH_3 produced in the H–B process is more cost effective despite the fact that this is actually a detour. Nitrogen in N_2 (oxidation state 0) is first reduced to ammonia (oxidation state −3), where after it is oxidized again to NO (oxidation state +2); in fact H_2 is burnt in this sequence to drive the overall reaction. Instead, a direct route from N_2 (oxidation state 0) to NO (oxidation state +2) in eqn (1) would be an elegant shortcut, which has the potential to be more efficient.

The H–B technology substantially increased the agricultural productivity and it succeeds in sustaining about 50% of the world population.[12] Nevertheless, the H–B process suffers from its poor scalability for decentralized production. Thus, industrial plants typically produce at least 100 t-NH_3 per day.[5] Furthermore, the H–B process operates at high temperatures and high pressures (350–500 °C and 100–300 bar), implying operation with varying load from intermittent renewables is difficult. Therefore, current research focuses on enabling load variation,[13] and on NH_3 synthesis under milder conditions.[14] Eventually, the H–B process may be replaced by a single-pass thermo-catalytic NH_3 synthesis process or electrochemical NH_3 synthesis.[15,16]

The emergence of low cost and intermittent renewable electricity may change the preferred choice of technology. Plasma technology offers potential benefits, such as fast turning on and off, and scalability for small communities.[9,17] The aim of this paper is to evaluate whether plasma-activated NO_X synthesis can become a feasible alternative for nitrogen fixation again in the 21st century, just like it was at the start of the 20th century. We identify how the state-of-the-art plasma nitrogen fixation process compares to the benchmark thermo-catalytic H–B process with the subsequent thermochemical Ostwald process. For this purpose, we will first explain the principles and state-of-the-art of the B–E process, the H–B process and the Ostwald process.

The Birkeland–Eyde process

The B–E process was the first nitrogen fixation process to operate commercially with hydropower in Niagara Falls (Canada). The power supplied to the B–E plant increased from 2.24 kW in 1903 to 238.6 MW in 1928. This commercial plant succeeded in fixing 38 kt-N $year^{-1}$.[2] About 175 t-air was required to fix 1 t-N *via* the B–E process.[9] The B–E process consumed about 2.4–3.1 MJ mol N^{-1} and produced 1–2 mol% NO.[9,17] A process scheme for the B–E process is shown in Fig. 2. Air was converted to NO in an electric arc formed between two coaxial, water-cooled copper electrodes placed between the poles of a strong electromagnet inside a furnace, for which various alternative configurations were considered.[9] Rapid quenching of the dilute nitrogen oxides to 800 – 1000 °C was applied at the reactor outlet to prevent reverse reactions (*i.e.*, converting NO back to N_2 and O_2).[2] The heat of the reaction was recovered

in waste heat boilers. Afterwards, oxidation of NO to NO_2 took place at a slow rate in a large oxidation chamber. Since the absorption capacity increases with decreasing temperature, the mixture of NO and NO_2 leaving the economizer at about 200 °C was further cooled to 50 °C in cooling towers before entering the absorption towers. Finally, NO_2 gas was absorbed in water to produce a solution of HNO_3. The final stream contained about 30% HNO_3 in water.[2] The un-absorbed NO_X was passed through alkaline absorption columns for further absorption. Despite this second absorption step, about 3% of the produced NO_X was purged to the atmosphere.

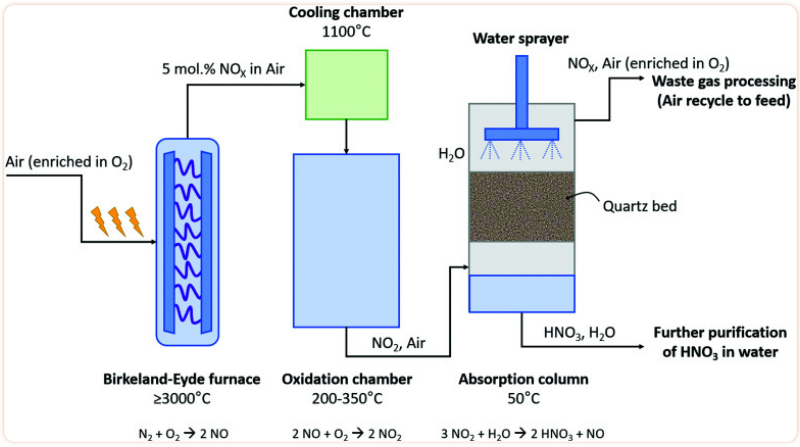

Fig. 2

Process scheme for the Birkeland–Eyde industrial nitrogen-fixation process. Inspired by Patil *et al.*[9]

Many ideas have been suggested to reduce the energy consumption of NO_X production and improve the performance of the B–E process, as for example the use of a 50–50% mixture of N_2 and O_2, preheating the inlet gas, applying heat recovery from process gas and operating the furnace at elevated pressures.[9] However, not only the plasma reactor is a major contributor to the investment and the energy cost of the B–E process, as also the absorption towers, especially the acid absorption towers, contribute significantly to the CapEx and OpEx.[18] According to a 1922 report on nitrogen fixation, the absorption columns compose over 40% of the CapEx and about 30% of the OpEx.[18] These absorbers were costly due to the low concentration of NO_X at the outlet of the plasma reactor. However, this technology has been optimized for the Ostwald process in previous decades, which could be used in combination with the B–E process as well. More recently, adsorbents, such as BaO, have been used to concentrate NO_X for car exhaust catalysts.[19] Through temperature swing adsorption (TSA) or pressure swing adsorption (PSA), the concentration of NO_X can be increased by using such solid sorbents. Possibly, such solid sorbents can replace or minimize the use of the costly absorption columns in the B–E process.

The Haber–Bosch process combined with the Ostwald process

In 1908, Haber and Le Rossignol demonstrated the feasibility of direct synthesis of 2 kg-NH_3 day^{-1} from N_2 and H_2 with a table top system operating at 500–550 °C and 100–200 atm, in the presence of an osmium catalyst.[1] In the following years, Mittasch and co-workers devel-

oped the multicomponent iron catalyst, a less poisonous and more abundant material, as an alternative to osmium for NH_3 synthesis,[20,21] while Bosch and co-workers solved engineering challenges regarding the operation with H_2 at high pressures.[22] In 1913, the first ammonia synthesis plant started operating according to the H–B process at BASF in Oppau, Ludwigshafen.[20] Nowadays, the H–B process starting from methane consumes about 0.5–0.6 MJ mol N^{-1}. This is the total energy content of the feed methane, of which about two third is transformed into hydrogen, while the remainder is used for heating during the steam methane reforming section for H_2 production, as discussed below.[23] The energy content of the ammonia product is only 0.32 MJ mol N^{-1}, implying significant heat generation during ammonia synthesis from methane. On the other hand, the H–B process starting from H_2O and N_2 also consumes about 0.5–0.6 MJ mol N^{-1} nowadays. The theoretical minimum energy consumption for NH_3 synthesis from H_2O and N_2 is 0.35 MJ mol N^{-1}. The overall yield of the H–B process is typically 97–99%, depending on the source of H_2 used.[15]

Schematic diagrams for a natural gas-based H–B process and an electrolysis-based H–B process are shown in Fig. 3. In the former method, H_2 is produced from methane (CH_4) *via* steam methane reforming (SMR), in which a mixture of CO, CO_2, and H_2 is produced. Typically, CH_4 is first converted with H_2O to CO and H_2 in a tubular reformer at 850–900 °C and 25–35 bar, after which the last portion of CH_4 conversion is performed by partial oxidation with air at 900–1000 °C, thereby introducing N_2 in the gas mixture. The CO is then converted with H_2O to CO_2 and H_2 in a two-stage water–gas-shift reactor, after which CO_2 is removed. Traces of CO are converted to CH_4 in a methanation step just before the synthesis loop, preventing deactivation of the ammonia synthesis catalyst. The feed gas, mainly composed of H_2 and N_2, is then compressed and fed to the ammonia synthesis loop operating at typically 100–300 bar, in which the reactants are fed to the ammonia synthesis reactor with iron-based catalysts operating at 350–500 °C. About 15–20% of the feed gas is converted to NH_3. The reactor effluent is then cooled down to ambient temperature to condense the NH_3 out. The remaining gas is recycled to the NH_3 synthesis reactor. This process scheme of NH_3 synthesis would be similar to the electrically-driven system. Here, H_2 is produced by electrolysis. Purified N_2 in the electrolysis-based process is produced in a separate unit by pressure swing adsorption (PSA) or cryogenic distillation.[14,24] Due to the different feedstocks for the SMR-based Haber–Bosch process and the electrolysis-based Haber–Bosch process, the heat integration between the process components changes substantially.

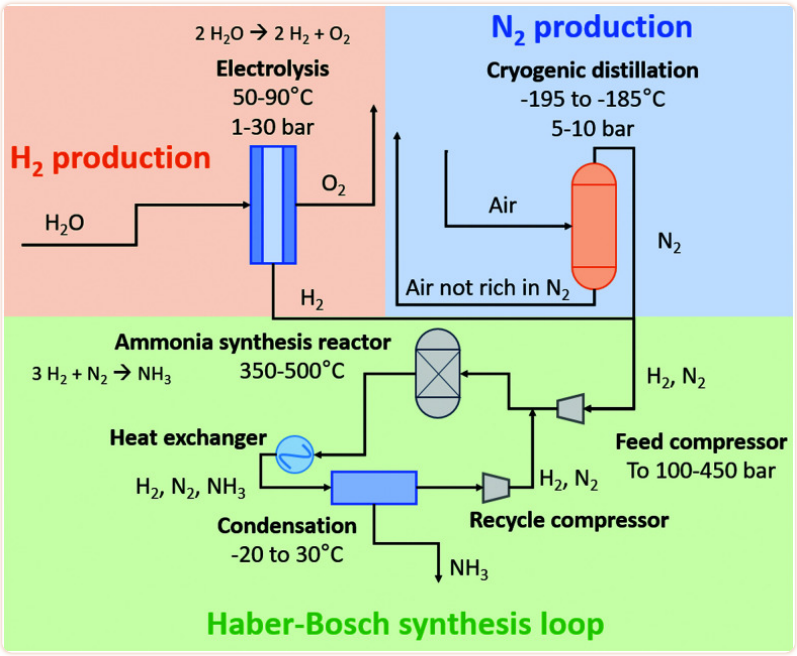

Fig. 3

Schematic diagram of the electrolysis-based Haber–Bosch process. For details, see text. Inspired by ref. 15.

The subsequent oxidation process was developed by Wilhelm Ostwald, who patented the ammonia oxidation process in 1902.[6] In this process, ammonia is oxidized in the presence of a rhodium–platinum gauze to form NO and H_2O at 600–800 °C and 4–10 atm. Afterwards, NO is cooled to about 50 °C and subsequently oxidized to NO_2 and absorbed in H_2O, producing dilute HNO_3. The untreated NO is recycled, while the HNO_3 is concentrated by distillation. The overall yield of the Ostwald process is typically 98%. A process scheme of the Ostwald process is shown in Fig. 4, which is similar to the B–E process (see Fig. 2), although less absorption steps are required due to the higher NO_2 concentration after the oxidation reactor.

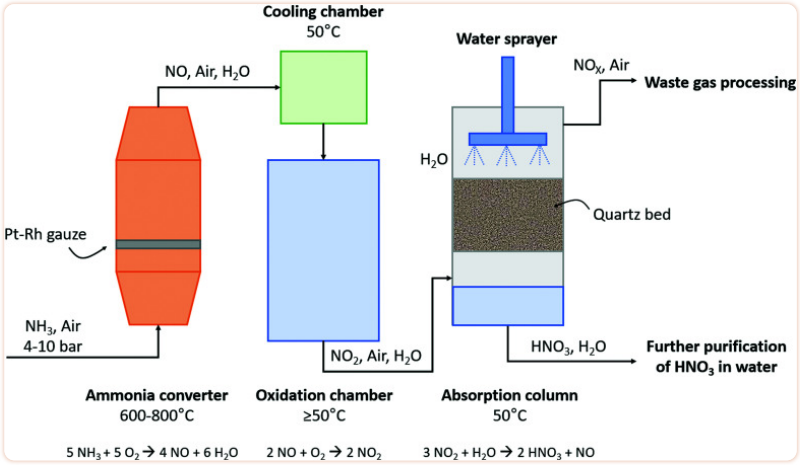

Fig. 4

Schematic diagram of the Ostwald process. For details, see text. Reproduced from ref. 25.

State-of-the-art of plasma-based NO_X synthesis

As discussed above, plasma-based NO_X synthesis was commercialized by Birkeland and Eyde in 1903,[26,27] and the energy consumed by the electric arc to generate a thermal plasma for NO synthesis is 2.4–3.1 MJ mol N^{-1}[7–9]. Hereafter we will discuss the state-of-the-art of plasma-based NO_X synthesis, as well as potential avenues for improvements.

Plasma types and comparison of energy consumption

Various plasma types can be distinguished, namely thermal plasmas, warm plasmas, and non-thermal plasmas. In a thermal plasma, the electrons and the heavier plasma species (molecules, radicals, and ions) are in thermal equilibrium, forming a quasi-neutral plasma bulk. The temperature in a thermal plasma is typically high (order of 10^4 K). The highest NO equilibrium concentration (about 5 mol%) can be achieved at a gas temperature near 3500 K and at 1 atm.[8] The NO formed is also prone to decomposition after the plasma, forming N_2 and O_2 again. Therefore, rapid quenching of the gas is required at a rate of several millions of Kelvins per second.[28,29] However, even if thermal plasma reactors are optimized, the theoretical minimum energy consumption for thermal plasmas is 0.72 MJ mol N^{-1}, which means that the energy efficiency of thermal plasma cannot compete with nitric acid produced from an electrolysis-based Haber–Bosch process (about 0.6 MJ mol N^{-1}). Here, the energy consumption refers to the electricity input for nitrogen fixation. The theoretical minimum energy consumption for thermal plasmas is based on the assumption that both N_2 and O_2 dissociate completely in the plasma, considering the bond-dissociation energies of N_2 (945 kJ mol^{-1}) and O_2 (498 kJ mol^{-1}).

In a non-thermal plasma, on the other hand, the electrons are not in equilibrium with the heavier plasma species, resulting in a substantially higher electron temperature as compared to the gas temperature, which is typically near room temperature. This potentially allows for selectively activating molecules with a strong chemical bond, such as N_2 (about 9.79 eV).[30] This is relevant for NO formation, as breaking the triple N ≡ N bond is rate-limiting for the formation of NO. The O_2 dissociation step takes place more easily, because of the somewhat weaker

O = O double bond (about 5.12 eV). Depending on the actual electron temperature, electrons can excite the molecules to various vibrational and electronic states. In typical non-thermal plasmas, such as dielectric barrier discharges (DBDs), the electron temperature is typically several eV, which mainly gives rise to electronic excitation.[17]

In between thermal and non-thermal plasmas, we can identify so-called warm plasmas, such as gliding arc (GA) and microwave (MW) plasmas, in which the electron temperature is still higher than the gas temperature, but the latter can be several 1000 K.[17] The electron temperature is typically 1–2 eV,[17] which is more beneficial for vibrational excitation of the molecules than in non-thermal plasmas (see eqn (7) for vibrational excitation). This gives rise to more efficient NO_X formation in warm plasmas.

Indeed, the NO formation rate *via* the reaction of atomic oxygen with N_2 by the so-called vibrationally-promoted Zeldovich mechanisms (eqn (8)) is enhanced upon increasing the population of N_2 vibrational levels in the plasma. The chain mechanism of NO synthesis is closed by the exergonic reaction given by Equation 9.[28,31] The sum of eqn (8) and (9) then gives a net energy consumption of 0.2 MJ mol N^{-1} for NO_X synthesis (*cf.* Table 1), *i.e.*, lower than NO_X synthesis *via* the electrolysis-based Haber–Bosch process combined with the Ostwald process. Therefore, exploiting the non-equilibrium phenomena in a plasma is a promising approach to increase the energy efficiency of plasma-based processes for nitrogen fixation.

Comparison of energy consumption for various production methods for nitric acid (best available technology, and minimum energy consumption). The best available technology refers to industrial practice and laboratory results. * See the ESI

Technology	Best available technology (MJ mol N^{-1})	Minimum energy consumption* (MJ mol N^{-1})
Thermochemical process (electrolysis-based Haber–Bosch + Ostwald)	0.6[15]	0.35[32]
Thermal plasma (Birkeland–Eyde process)	2.4–3.1[7–9]	0.72
Warm plasma (Gliding arc reactor)	2.4[33]	0.5[34]
Plasma with only vibrationally-promoted Zeldovich mechanism (only vibrational excitations in N_2)	—	0.2[8]

It should also be noted that unproductive electronic excitation and ionization channels in real plasma reactors lead to a higher minimum energy consumption than for an hypothetical plasma reactor operating exclusively *via* the vibrationally-promoted Zeldovich mechanism (eqn (8)). The distribution of productive and unproductive N_2 activation channels leads to a theoretical minimum energy consumption of about 0.5 MJ mol N^{-1} (see Table 1) for a gliding arc plasma reactor, which is a warm plasma type.[28,33,34] The different plasma activation channels for N_2 and O_2 in various plasma reactors are shown in Fig. 6.

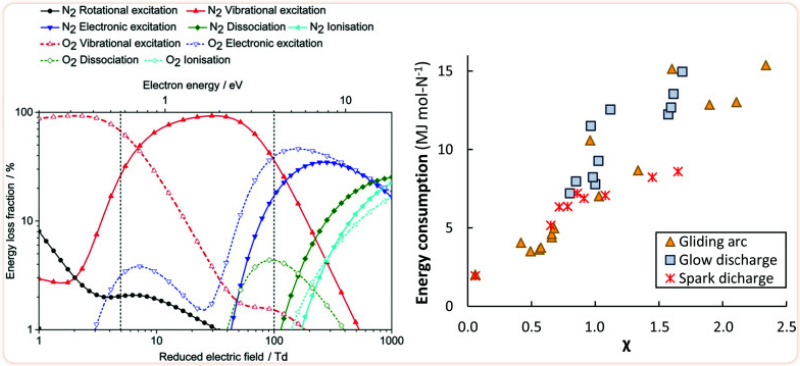

Fig. 6

Left: The dominant plasma-activation channels in 50 : 50 N_2 : O_2 stream. Reproduced from ref. 62. Reduced electric fields of 5–100 T_d correspond to GA and MW plasmas, while the region above 100 T_d corresponds to a DBD reactor.[17] Right: The apparent energy cost as function of the χ factor, as proposed by Pei *et al.*[53] Original reference: gliding arc,[34,53,62,80,81,91–95] glow discharge,[53] spark discharge.[53,54]

In practice, the energy consumption is even higher, which is due to vibrational–translational relaxation (hence depopulating the N_2 vibrational levels), and NO_X decomposition after the plasma if the temperature does not drop fast enough. Plasma radicals may also recombine to form O_2 and N_2 again, implying all energy is lost as heat. Lastly, decomposition of NO_X products in the plasma will further limit the energy efficiency. With increasing NO_X concentration, the probability of plasma-activation of NO_X increases, thereby promoting the reaction back to N_2 and O_2.

$$e^- + N_2 \rightarrow e^- + N_2(v). \quad (7)$$

$$O + N_2(v) \rightarrow NO + N. \quad (8)$$

with $E_a \approx \Delta H_r \leq 3$ eV per molecule (note: 3 eV is the barrier for a ground-state N_2 molecule, and the barrier decreases upon increasing vibrational excitation of N_2)

$$N + O_2 \rightarrow NO + O. \quad (9)$$

with $E_a \approx 0.3$ eV per molecule and $\Delta H_r \approx -1$ eV per molecule[28]

The enthalpy of formation for NO is 90 kJ mol N^{-1} and any addition of energy input above that level leads to the formation of heat. Thus, even in case of the Zeldovich mechanism with an energy consumption of 0.2 MJ mol N^{-1}, 55% of the energy in the reactor is lost as heat. In case of thermal dissociation of the triple N ≡ N bond (945 kJ mol^{-1}) and double O = O bond (498 kJ mol^{-1}), only 12% of the energy is stored in the N = O bond whereas 88% in converted to heat.

Plasma catalysis

A potential avenue to improve the energy efficiency of the process beyond optimizing the plasma is the introduction of a catalyst. Catalysts are used in most chemical processes to decrease the reactor size, as well as to operate at milder operating conditions and to lower t energy requirement. Various authors have attempted the use of metal and metal oxide catalysts for plasma-based NO_X synthesis.[35,36] However, up till now, results are inconclusive on whether there is an actual catalytic effect rather than a change in the physiochemical plasma properties d to the introduction of a packing material into the reactor.[8,36,37] A change of packing material is known to modify the plasma properties, and thereby the conversion.[38] Some synergistic effects between plasma and catalyst have however been proposed. Rapakoulias *et al.*[35] investigated NO synthesis in the presence of transition metal oxides, such as molybdenum trioxide (MoO_3) and tungsten trioxide (WO_3) catalysts (*e.g.* n-type semiconductors). The authors proposed that the vibrationally excited N_2 molecules undergo dissociative adsorption on the catalytic surface (eqn (10)). This may occur because n-type semiconductors donate electrons because of their easy ionization. Therefore, the adsorbed molecule can accept electrons to its anti-bonding π* orbital, leading to its pre-dissociation.[39] Then, the atomic nitrogen may react with surface oxygen, forming NO upon desorption (eqn (11)). The oxygen vacancy can then be replenished by oxygen from the gas phase (eqn (12)), thereby oxidizing the transition metal surface, according to a Mars–van Krevelen redox mechanism.[40]

$$N_2(v) \xrightarrow{\text{surface}} 2N_{\text{ads}}\cdot \quad (10)$$

$$N_{\text{ads}} + O \xrightarrow{\text{surface}} (NO)^*_{\text{ads}} \xrightarrow{\text{desorption}} NO + {}_{\text{vac}}\cdot \quad (11)$$

$$\text{vac} + \frac{1}{2}O_2 \rightarrow O_{\text{surface}}\cdot \quad (12)$$

It should be noted, however, that the dissociative sticking probability of N_2 is probably very low on oxide surfaces, even upon substantial activation of N_2*via* vibrational or electronic excitation. The dissociative sticking probability on Ru(0001), a metal that has thermal activity for N_2 dissociation, for N_2 pre-activated with 300–400 kJ mol^{-1} is as low as 10^{-3}–10^{-2}[41,42]. For W(110), a metal that is much less noble, the dissociative sticking probability is only 0.35 upon pre-activation of 100 kJ mol^{-1}[43]. As oxides are much less able to dissociate N_2 compared to metals, the

sticking probability of N_2 on oxides is even much lower, so most of the collisions of activated N_2 molecules with the oxide surface will lead to energy relaxation instead of N_2 dissociation. This will be a major pathway for energy loss.[44]

A limitation of a thermally-active catalyst is that it always catalyses not only the NO_X synthesis reaction but also the reverse decomposition reaction.[45] As the equilibrium at mild conditions is completely towards the formation of N_2 and O_2, a metal catalyst with thermal catalytic activity will in principle mainly form N_2 and O_2 under mild conditions.[46] The presence of a surface could improve the performance only if it would enhance an irreversible reaction step, *e.g.* a quenching reaction of a highly activated species, leading to the formation of NO_X.[47] This can potentially be achieved with metal oxide catalysts, or metals inactive for NO_X decomposition such as Ag and Au. However, at ambient temperatures, a catalytic effect was not observed for NO_X synthesis on alumina-supported W-, Co- and Pb-oxides in a dielectric barrier discharge (DBD) reactor,[36] and any change in activity must be attributed to modifications in the physiochemical plasma properties due to the introduction of a packing material into the reactor. On the other hand, metal oxides become active for NO decomposition at elevated temperatures.[45,48–50]

Performance of various plasma reactors

Various plasma types and plasma reactors have been investigated for NO_X production after the earlier research on thermal plasma (*i.e.*, the electric arc).[26,27,33,51] This includes spark discharges,[52–55] radio-frequency crossed discharge,[56] laser-produced discharge,[57] corona discharges,[52,58] glow discharges,[53,59] (packed bed) dielectric barrier discharges (PB) DBD,[36,53] (pulsed) (gliding) arc discharges,[34,53,60–62] microwave (MW) discharges,[63–65] and plasma jets in contact with water.[66–76]

A summary of the reported energy consumption and the product concentration in various plasma reactors is listed in Table 2. Additionally, the reported NO_X concentration and energy consumption are shown in Fig. 5. A distinction is made between various types of plasma reactors.

Comparison of energy consumption for NO production in various plasma reactors

Plasma type	Product (concentration)	Energy cost (MJ mol N^{-1})	Ref.
Electric arc (Birkeland–Eyde)	NO (2%)	2.4–3.1	26,27,51
Spark discharge	NO and NO_2	20.27, 40	52,55
Transient spark discharge	NO and NO_2	8.6	54
Pin-to-plane ns-pulsed spark discharge	NO and NO_2	5.0–7.7	53
Radio-frequency crossed discharge	HNO_3	24–108	56
Laser-produced discharge	NO and NO_2	8.9	57
(Positive/negative) DC corona discharge	NO and NO_2	1057/1673	52
Pulsed corona discharge	HNO_3	186	58
Pin-to-plane DC glow discharge	NO and NO_2	7	53
Pin-to-pin DC glow discharge	NO and NO_2 (0.7%)	2.8	59
Dielectric barrier discharge	NO and NO_2 (0.6%)	56–140	53
Packed dielectric barrier discharge	NO and NO_2 (0.5%)	18	36
DC plasma arc jet	NO (6.5%)	3.6	60
Propeller arc	NO and NO_2 (0.4%)	4.2	53
Pulsed milli-scale gliding arc	NO and NO_2 (1–2%)	2.8–4.8	61,62
Gliding arc plasmatron	NO and NO_2 (1.5%)	3.6	34
Rotating gliding arc	NO and NO_2 (5.4%)	2.5	33
Microwave plasma	NO and NO_2 (0.6%)	3.76	63
Microwave plasma with catalyst	NO (6%)	0.84	64
Microwave plasma with magnetic field	NO (14%)	0.28	65

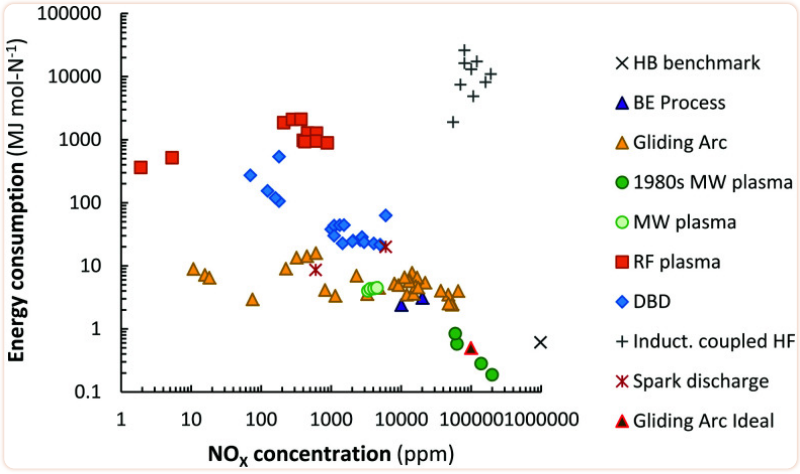

Fig. 5

Comparison of energy consumption for NO production in various plasma reactors. Original references: 1980s low pressure MW plasma,[64,65,77,78] MW plasma,[63] gliding arc,[33,34,53,60,62,79–82] RF plasma,[83,84] DBD,[36,53,85,86] inductively coupled HF,[35] spark discharge.[54,55]

Among the different plasma types, warm plasmas, such as gliding arcs (GA), atmospheric pressure glow discharges (APGD) and microwave plasmas (MW), have been explored extensively for gas conversion applications.[17] As explained above, warm plasmas are a special type of plasma that include both thermal and non-thermal plasma characteristics. The gas temperature is typically a few 1000 K, while the electron temperature is still higher (1–2 eV), thus, providing warm plasmas with non-equilibrium (or non-thermal) characteristics. However, the vibrational temperature is (nearly) equal to the gas temperature, resulting in vibrational–translational (VT) equilibrium.[87,88] Therefore, warm plasmas are also known as quasi-thermal plasmas.

Different GA reactor configurations have shown promise for gas conversion applications.[17,34,61,62,89,90] GA plasmas are characterized by reduced electric fields below 100 Td, resulting in electron energies around 1 eV. Such electron energies are most beneficial for vibrational excitation of the gas molecules (see Fig. 6a).[17] Wang *et al.*[62] investigated NO_X formation mechanisms in a pulsed-power milliscale GA reactor, while Vervloessem *et al.*[34] studied NO_X formation in a reverse-vortex flow gliding arc plasmatron (GAP). The chemical kinetics modelling results showed that the vibrationally excited N_2 molecules can reduce the energy barrier of the non-thermal Zeldovich mechanism $O + N_2(v) \rightarrow NO + N$, providing an energy-efficient way for NO production.

Moreover, the high gas temperature (>3000 K) leads to significant thermal dissociation of the lower N_2 vibrational levels, whose vibrational distribution function exhibits a Boltzmann shape. In fact, thermal reactions are quite efficient at the high temperatures reached in GA reactors. The limitation in the overall N_2 conversion is rather the fraction of gas treated by the GA plasma. For instance, only 15% of the gas is estimated to pass through the plasma arc in the GAP and the rest of the gas by-passes through the reactor without contacting the plasma.[90,96] Vervloessem *et al.*[34] reported a NO_X yield of 1.5% at an energy consumption of 3.6 MJ mol N^{-1}.

Through reactor optimization and by preventing the transfer of vibrational energy from N_2 to O_2, the authors showed that the energy consumption can potentially decrease to 0.5 MJ mol N^{-1}.[34]

Janda *et al.*[54] studied NO_X production in a transient spark discharge. This type of spark discharge starts from a streamer phase, *i.e.* a non-thermal plasma, and is subsequently transformed into short spark current pulses which generate a thermal plasma. The self-pulsing feature of the discharge avoids thermalization of the plasma.[97,98] The spark phase is characterized by a high chemical activity due to the high electron density achieved (about 10^{17} cm^{-3}). The excited nitrogen molecules (N_2*) were observed in both the streamer and the spark phases and the energy consumption for NO_X production was 8.6 MJ mol N^{-1}[54]. Pavlovich *et al.*[55] developed a spark-glow discharge reactor, where the generated plasma discharge had a spark phase (thermal plasma) and glow phase (non-thermal plasma) in one cycle. The authors were able to control the percentage of glow phase by fine-tuning the voltage waveforms. The spark phase, which had a very high electron density and energy, generated more NO, while the glow phase promoted the oxidation of NO to NO_2. However, the energy consumption of NO_X production was as high as 40 MJ mol N^{-1}. In general, such plasma types have a limited volume, resulting in a limited fraction of the N_2 gas being exposed to the plasma, and thus a limited amount of NO_X produced.

Packed bed DBD reactors have also been studied, because of the possibility to enhance the product selectivity and the energy efficiency by combining the plasma with a catalyst. Patil *et al.*[36] studied NO_X production in a DBD packed with different catalyst support materials (α-Al_2O_3, γ-Al_2O_3, TiO_2, MgO, $TaTiO_3$, and quartz wool). The authors obtained the best results with a γ-Al_2O_3 catalyst with the smallest particle size of 250–160 μm. However, the obtained energy cost was high (18 MJ mol N^{-1}) and the product yield low (0.5 mol%), compared to other atmospheric pressure plasma reactors.[36] These poor results obtained in a DBD could be explained by the high reduced electric field, *i.e.* above 100–200 T_d, which creates highly energetic electrons, resulting mainly in electronic excitation, ionization, and dissociation, instead of vibrational excitation (see Fig. 6a), and thus not exploiting the most energy-efficient NO_X formation pathway through the vibrationally-induced Zeldovich mechanism.[17]

The best results in terms of product yield and energy consumption were obtained in low-pressure MW plasmas. The energy consumption obtained in a MW plasma with catalyst was stated to be 0.84 MJ mol N^{-1} for an NO concentration of 6 mol%.[64] The highest NO concentration of 14% and lowest energy cost of 0.28 MJ mol N^{-1} were reported for a MW plasma with magnetic field (so-called electron cyclotron resonance).[65] However, these values were reported in the 1980s and have not been reproduced in recent years. A similar situation exists for plasma-based CO_2 splitting, where results from the 1980s could not be reproduced with similar reactors in recent years.[99] Therefore, the reported energy yield calculations for plasma-based NO_X synthesis in a MW plasma from the 1980s should be assessed critically.

These MW plasmas operated at reduced pressures (down to 66 mbar), which indeed promote vibrational–translational non-equilibrium, and thus the vibrational-induced Zeldovich mechanisms. Hence, this partially explains their high product yields and low energy consumption. However, the low reported energy consumptions only account for the plasma power and do not include the energy consumed by both the vacuum equipment and the reactor cooling sys-

tem. Therefore, the overall energy cost of NO_X production in a MW plasma would be higher. Operation of MW reactors at higher pressures is also possible, but heat losses increase due to increased collision frequency.[100]

In 2010, Kim *et al.*[63] reported a performance of 3.76 MJ mol mol N^{-1} and 0.6% NO_X, similar to that of GA reactors, but for a MW plasma at a pressure slightly below atmospheric and for an input power between 60 and 90 W and at a fixed flow rate of 6 L min^{-1} (see Fig. 5). Power pulsing in a MW reactor may suppress unfavourable vibrational–translational relaxation, hence increasing the vibrational temperature, and thus the vibrational–translational non-equilibrium, needed for (the most energy-efficient) vibration-induced dissociation of N_2.[101]

Pei *et al.*[53] investigated four different plasma types, *i.e.* DBD, glow, spark and arc-type, and identified a key parameter (so-called χ factor, eqn (13)) that appeared to correlate the energy cost of NO_X production with a range of different discharges (see Fig. 6b). The authors showed that NO_X production efficiency can mainly be controlled by the average electric field and the average gas temperature of the discharge.

$$\chi = \frac{\bar{E} \times \bar{T}}{E_r \times T_r}. \quad (13)$$

Therefore, they defined the dimensionless parameter by eqn (13), where $\bar{E}$ (kV cm^{-1}) and T (K) are the average electric field and average gas temperature of the discharge under study, respectively, while E_r. (*i.e.* 1.43 kV cm^{-1}) and T_r (*i.e.* 1800 K) are chosen to normalize the parameter to a reference condition. The authors chose a DC glow discharge with a gap of 5 mm and a discharge current of 45 mA as a reference condition because of its simplicity and stability, *i.e.* the discharge conditions can be easily reproduced for reference. By decreasing the χ factor, *e.g.* by decreasing the electric field and/or the average gas temperature of the discharge, the energy cost can be reduced. The two important mechanisms that control the energy efficiency of NO_X production in any type of discharge are (i) efficient electron-impact activation of N_2 molecules to facilitate NO_X formation, which is influenced by the electric field, and (ii) rapid thermal quenching of NO to prevent its conversion back to N_2 and O_2 molecules when the gas temperature drops more slowly. N atoms formed at high electric fields are an important pathway for NO_X decomposition.[62] The authors suggested various methods to decrease the average gas temperature, such as cooling the reactor walls with water, using short duration high current pulses, and extending t discharge length.[33]

Finally, NO_X production has also been reported by plasma jets flowing in (ambient) air (or N_2 atmosphere), and interacting with water.[66–76] Generally, the focus of this research was on NH_3/NH_4^+ formation, but NO_2^- and NO_3^- formation was also reported, due to the presence of

oxygen. The combination of plasma jets and water potentially allows for removal of the product NO_X, thereby preventing its decomposition by the plasma.

Comparison of direct plasma-based NO_X synthesis and the Haber–Bosch process combined with the Ostwald process

In this section, we assess the techno-economic feasibility of a direct plasma-based NO_X synthesis process with subsequent conversion to HNO_3, in comparison to an electrolysis-based Haber–Bosch process combined with the Ostwald process for HNO_3 production. Both processes produce nitric acid from water, air, and electrical power exclusively. To the best of our knowledge, direct cost analyses comparing the direct plasma-based NO_X synthesis process and the H–B process combined with the Ostwald process have not been reported yet.[2,102]

The production capacity considered is 100 t-HNO_3 day^{-1}, *i.e.* a factor 1000 smaller than world-scale Haber–Bosch plants, at an electricity cost of 20 € MW h^{-1}. The cases considered are (1) the electrolysis-based Haber–Bosch process combined with the Ostwald process (EHB + O base-case), (2) the plasma-based NO_X synthesis process at an energy cost of 2.4 MJ mol N^{-1} (PL base-case, based on the recent results of Jardali *et al.*[33] for gliding arc plasmas), and (3) the potential plasma-based NO_X synthesis process at an energy cost of 0.5 MJ mol N^{-1} (PL potential). The energy consumption of 0.5 MJ mol N^{-1} is based on the theoretically minimum attainable energy consumption in a gliding arc reactor,[34] as listed in Table 1.

Capital expenditure

The capital expenditure for the electrolysis-based Haber–Bosch process and the Ostwald process (*e.g.*, the EHB + O base-case) is estimated from cost-scaling relations.[103,104] The capital expenditure for the plasma-based NO_X synthesis process (PL) is estimated from the cost-scaling relations for the Ostwald process, and from reported costs of plasma reactors. The current estimated cost for the plasma-reactor is 0.90 € W^{-1}, based on a recent estimate of Van Rooij *et al.*[105] for microwave reactors, as well as the cost of power supplies for DBD reactors (about 1.00–2.00 € W^{-1} for a few hundreds of W). The estimated cost for plasma generators is expected to decrease to 0.05 € W^{-1} for large-scale application.[105]

A comparison of the capital expenditure for the electrolysis-based Haber–Bosch process, combined with the Ostwald process, and the plasma-based NO_X synthesis process is shown in Fig. 7. The 'high' case and 'low' case refer to a plasma generator cost of 0.90 € W^{-1} and 0.05 € W^{-1}, respectively. As shown in Fig. 7, the cost of a PL base-case is nearly on par with the EHB + O base-case. Upon improving the energy consumption from 2.4 MJ mol N^{-1} to 0.5 MJ mol N^{-1} or upon decreasing the cost of the plasma generator, the capital expenditure of the plasma-based process is about half to one third that of the EHB + O base-case. Thus, the plasma-based NO_X synthesis process has potentially a highly competitive capital expenditure, especially when the cost of the plasma generator becomes as low as 0.05 € W^{-1}.

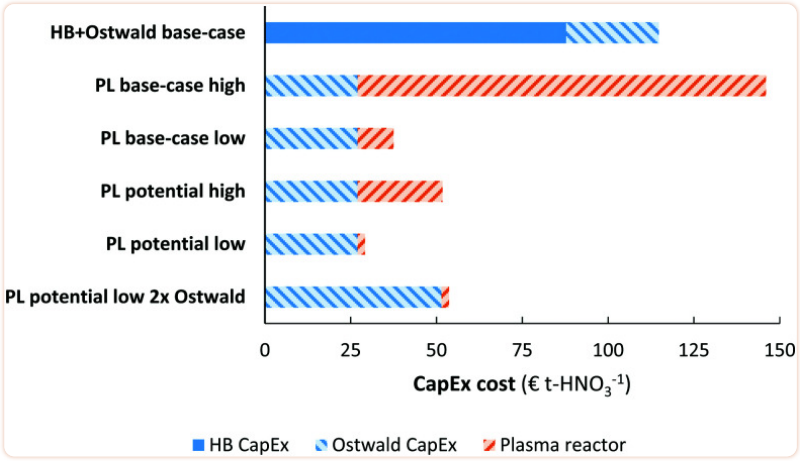

Fig. 7

Comparison of the capital expenditure for various HNO_3 synthesis methods. Cost-scaling numbers from ref. 103 for the electrolysis-based Haber–Bosch process, from ref. 104 for the Ostwald process, and ref. 105 for the plasma reactor. See text for more information. The annuity is assumed to be 10%.

We assumed that the CapEx for the plasma process is similar to that of the Ostwald process (apart from the plasma reactor), due to the similarity in the downstream NO_X absorption steps. However, the NO_X concentration may be lower in case of plasma-based NO_X synthesis (see Fig. 5). Therefore, an additional unit operation may be required to concentrate the produced NO_X for the plasma-based NO_X synthesis process. Therefore, we also show the CapEx for the plasma-based NO_X process (PL) with double the equipment required for downstream NO_X absorption and conversion to HNO_3. As shown in Fig. 7, the CapEx of the PL process is lower, even if twice the equipment capacity is required for the NO_X absorption in the PL process as compared to the EHB + O base-case process.

Effect of energy consumption

The energy consumption is another important descriptor for the operational cost of a process (see Fig. 8). The cases presented in Fig. 7 are also shown in Fig. 8a. It is clear that the energy consumption has a major impact on the total cost of HNO_3 production, and a minor increase in the capital expenditure has little effect on the overall economics on the process. Thus, it is reasonable to focus on the energy consumption of the process.

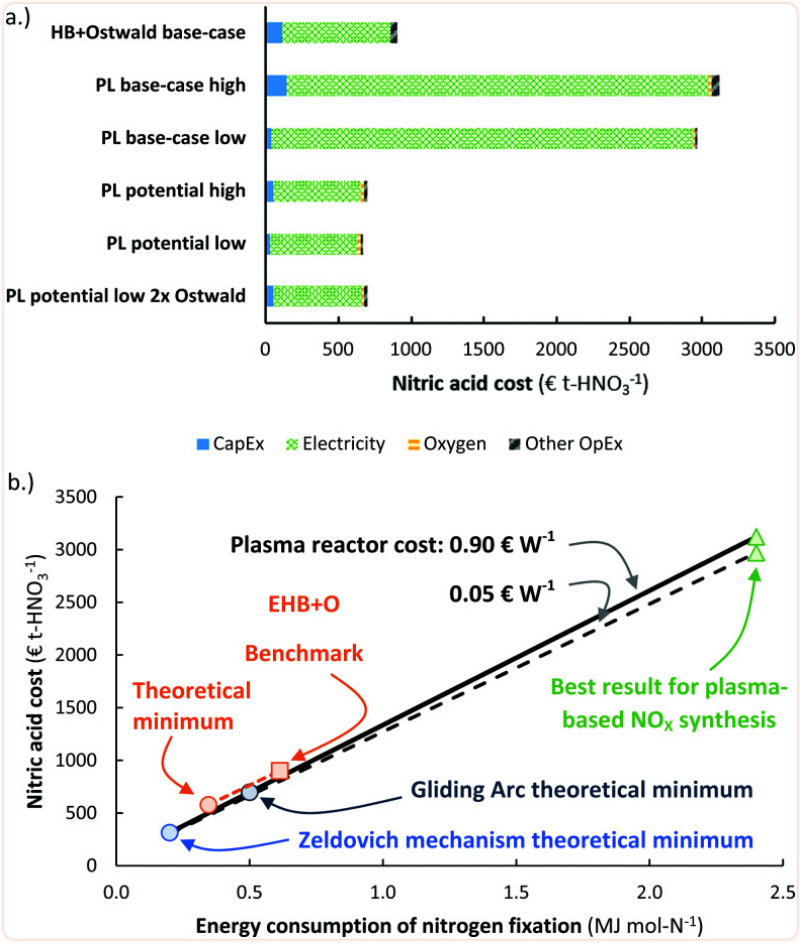

Fig. 8

(a) Cost breakdown of the total cost of nitric acid production, for the cases considered in Fig. 7. The 'high' case and 'low' case refer to a plasma generator cost of 0.90 € W^{-1} and 0.05 € W^{-1}, respectively. Process capacity 100 t-HNO_3 day^{-1}, electricity cost 20 € MW h^{-1}. Oxygen is added to account for the lower oxygen content in air, as compared to the nitrogen content in air. At the process scale of 100 t-HNO_3 day^{-1}, about 1300 m^3-O_2 h^{-1} is required, which costs about 14–28 € t-HNO_3^{-1}.[106] The operational costs apart from the electricity cost is assumed to be 2% of the CapEx. (b) Effect of the energy consumption of the plasma-based NO_X synthesis process on the total cost of nitric acid production. The solid and dotted line represent the plasma process with a plasma reactor cost of 0.90 € W^{-1} and 0.05 € W^{-1}, respectively. The orange square represents the total cost of nitric acid for a reference electrolysis-based Haber–Bosch process combined with an Ostwald process. Process capacity 100 t-HNO_3 day^{-1}, electricity cost 20 € MW h^{-1}.

The effect of the energy consumption on the nitric acid cost in the plasma-based NO_X synthesis process is shown by the solid and dotted lines in Fig. 8b, from which it follows that the plasma-based NO_X synthesis process becomes competitive with the electrolysis-based Haber–Bosch process combined with the Ostwald process at an energy consumption of 0.7 MJ mol N^{-1}. As listed in Table 1, this is not attainable for thermal plasmas, as these plasmas have a minimum energy consumption of 0.72 MJ mol N^{-1}. However, warm plasmas may attain the required energy consumption below 0.7 MJ mol N^{-1} (see Table 1).

Effect of electricity cost & process capacity

It should be noted that the current market value of HNO_3 is about 250–350 € t-HNO_3^{-1}, while the predicted cost of HNO_3 production for the EHB + O base-case and the PL potential low cases is as high as 890 € t-HNO_3^{-1} and 655 € t-HNO_3^{-1} for an electricity cost of 20 € MW h^{-1}. The relatively low market value of HNO_3 is mainly due to the low cost of fossil-based feedstocks, such as natural gas and coal.[107] As shown in Fig. 8b, the CapEx only has a minor effect on the total cost of HNO_3 production at the process scale considered (100 t-HNO_3 day^{-1}). Thus, the cost of electricity is a common descriptor for sustainable HNO_3 production from the electrolysis-based Haber–Bosch process combined with the Ostwald process and the plasma-based NO_X synthesis process, as compared to fossil-based HNO_3 production.

The cost of nitric acid production as function of the electricity cost is shown in Fig. 9. It is immediately clear that chemicals produced with electricity require low electricity cost (<5–10 € MW h^{-1}) in order to become cost-competitive with fossil-based HNO_3 production. The lowest solar auction prices in recent years are in the range 15–20 € MW h^{-1}, implying the electricity-driven processes may become competitive with fossil-based processes in the upcoming decades.

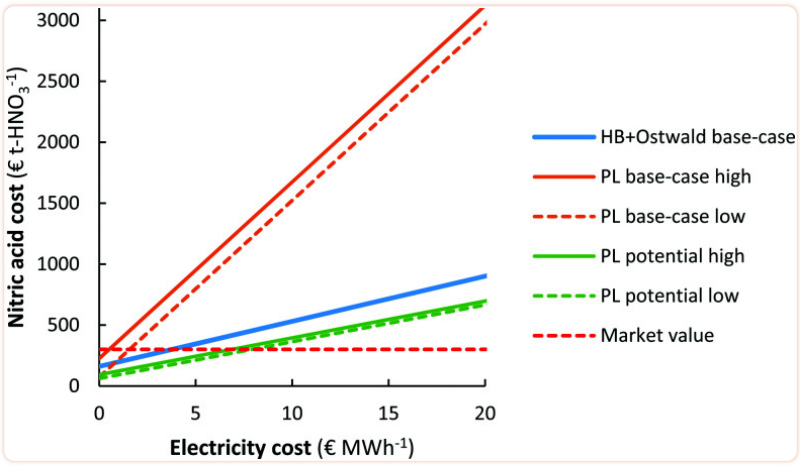

Fig. 9

Effect of the electricity cost on the cost of nitric acid production. Process capacity 100 t-HNO_3 day^{-1}. The same cases are considered as in Fig. 7.

It should be noted, however, that the cost of HNO_3 depends on the geographic location. While the market value is as low as 250–350 € t-HNO_3^{-1} in some locations where the cost of transportation is minimal, the cost at remote locations (*e.g.*, the interior of sub-Saharan Africa) can be multiple times that of the production cost[108,109] so that electricity driven processes may become favourable at higher electricity cost.

Effect of process capacity

As shown in Fig. 10, the plasma-based NO_X synthesis process has the benefit over the Haber–Bosch process combined with the Ostwald process that the capital expenditure for ammonia synthesis is not required. This means there is potential for decentralized HNO_3 synthesis, instead of importing HNO_3 to remote locations.[109] While the Haber–Bosch process suffers from

a high CapEx upon scale-down to capacities below 50 t-HNO_3 day^{-1}, the plasma-based NO_X synthesis process may be scaled down more effectively (see Fig. 10). Hence, plasma-based NO_X synthesis may be used for decentralized nitrogen fixation. It should be noted, however, that scale-down below 1 t-HNO_3 day^{-1} also becomes less economical for the plasma-based NO_X synthesis process, due to an increase in oxygen purification cost upon scale-down.[106]

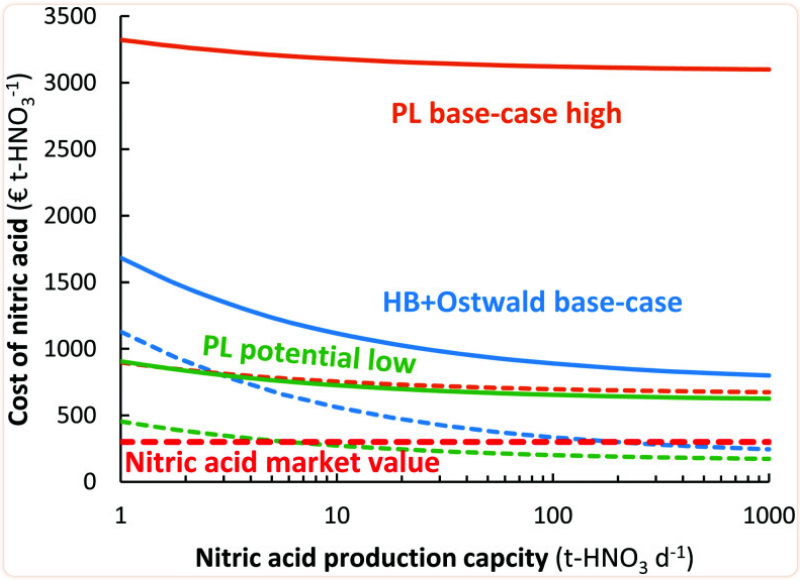

Fig. 10

Effect of nitric acid production capacity on the cost of nitric acid for the electrolysis-based Haber–Bosch process combined with the Ostwald process, as well as for the plasma-based NO_X synthesis process. The full and dotted lines represent an electricity cost of 20 € MW h^{-1} and 5 € MW h^{-1}, respectively. The high pressure Haber–Bosch process becomes less energy-efficient upon scale down below 10 t-HNO_3 day^{-1}.[14,110] The HB + Ostwald base-case, PL base-case, and PL potential case are the same as in Fig. 8.

Further improving the performance of plasma-based NO_X synthesis

In recent years, various studies have reported on combination of experimental and modelling work for plasma-based NO_X synthesis.[33,34,62,91] This has improved the understanding of the dominant reaction pathways in real plasma reactors under relevant reaction conditions. However, the energy cost of plasma-based NO_X synthesis remains higher than for the benchmark electrolysis-based Haber–Bosch process combined with the Ostwald process (see Fig. 5). Thus, further performance improvement is required, beyond optimizing experimental conditions, *e.g.* inspired by modelling.

Modelling can, however, also help to improve the reactor design to improve the contacting of gas with plasma so that a larger fraction of gas actually passes through the plasma. This is now often a limitation in for instance gliding arc plasma reactors,[34,99] thus limiting the overall gas conversion. Such modelling can describe gas flow dynamics, arc plasma behaviour and plasma

chemistry, tracing the gas molecules through the reactor. This allows evaluation of the exact plasma conditions to which molecules are exposed, resulting on optimal conversion by the plasma, as recently demonstrated.[33,111]

Besides enhancing the gas fraction passing through the plasma, attention should also be paid to fast quenching, *i.e.* cooling, of the gas downstream of the plasma, avoiding the backward reaction, *i.e.* decomposition of NO_X to N_2 and O_2. The major beneficial effects of fast quenching were recently studied in detail for CO_2 conversion in plasma,[112] but the same principle also applies to NO_X synthesis. In addition, heat integration is required, using the heat released during gas cooling for pre-heating the gas before entering the plasma reactor,[82].

Finally, as discussed in Section 2.2, catalytic enhancement of plasma-based NO_X synthesis is an option to increase the NO_X yield at the same energy input. Such materials should not catalyse the decomposition of NO_X molecules, as this would even decrease the NO_X yield as compared to pure plasma-based NO_X synthesis. Secondly, the use of NO_X sorbents may be beneficial. Removal of NO_X species from the plasma environment may prevent the subsequent decomposition of the product by the plasma. Catalyst particles or sorbent particles may be introduced in or after the plasma reactor as a fixed bed, a trickle bed, or a fluidized bed.

Conclusion

We have evaluated the state-of-the-art for plasma-based NO_X synthesis. From a techno-economic analysis, it follows that plasma-based NO_X synthesis is potentially viable for electricity-based HNO_3 production. As compared to the electrolysis-based Haber–Bosch process combined with the Ostwald process, the plasma-based NO_X synthesis process benefits from a lower capital expenditure. The current energy cost of ≥2.4 MJ mol N^{-1}[91] is however still too high to be competitive with the electrolysis-based Haber–Bosch process combined with the Ostwald process, which consumes about 0.6 MJ mol N^{-1}[15]. Plasma-based NO_X synthesis will become a highly-competitive alternative to the Haber–Bosch process combined with the Ostwald process, if the energy consumption can be decreased to 0.7 MJ mol^{-1} *via* smart reactor design, tuning the chemistry and vibrational kinetics, avoiding back-reactions, or combination with catalysts. Thus, plasma technology may become an effective turnkey technology compatible with intermittent electricity.[113]

Conflicts of interest

There are no conflicts to declare.

Acknowledgments

This research was supported by the TKI-Energie from Toeslag voor Topconsortia voor Kennis en Innovatie (TKI) from the Ministry of Economic Affairs and Climate Policy, the Excellence of Science FWO-FNRS project (FWO grant ID GoF9618n, EOS ID 30505023), and the European Research Council (ERC) under the European Union's Horizon 2020 research and innovation programme (grant agreement No 810182 – SCOPE ERC Synergy project).

References

1. Travis A. S., *Nitrogen Capture: The Growth of an International Industry (1900–1940)*, Springer International Publishing, 2018 10.1007/978-3-319-68963-0 [CrossRef] [Google Scholar]
2. Ernst F. A., *Industrial Chemical Monographs: Fixation of Atmospheric Nitrogen*, London, UK: Chapman & Hall, Ltd, 1928 [Google Scholar]
3. Travis A. S., *The Synthetic Nitrogen Industry in World War I: Its Emergence and Expansion. The Synthetic Nitrogen Industry in World War I*, 2015 10.1007/978-3-319-19357-1 [CrossRef] [Google Scholar]
4. Smil V., *Enriching the Earth: Fritz Haber, Carl Bosch, and the Transformation of World Food Production*, Cambridge, MA, 2004 [Google Scholar]
5. Brightling J. R. Ammonia and the fertiliser industry: The development of ammonia at Billingham. *Johnson Matthey Technol. Rev.* 2018;62(1):32–47. doi: 10.1595/205651318X696341. [CrossRef] [Google Scholar]
6. Thiemann M., Scheibler E. and Wiegand K. W., Nitric acid, nitrous acid, and nitrogen oxides, in *Ullmann's Encyclopedia of Industrial Chemistry*, 2000 10.1002/14356007.a17_293 [CrossRef] [Google Scholar]
7. Rouwenhorst K. H. R., Krzywda P. M., Benes N. E., Mul G. and Lefferts L., Ammonia, 4. Green Ammonia Production, in *Ullmann's Encyclopedia of Industrial Chemistry*, 2020 10.1002/14356007.w02_w02 [CrossRef] [Google Scholar]
8. Cherkasov N. Ibhadon A. O. Fitzpatrick P. A review of the existing and alternative methods for greener nitrogen fixation. *Chem. Eng. Proc.: Proc. Intens.* 2015;90:24–33. doi: 10.1016/j.cep.2015.02.004. [CrossRef] [Google Scholar]
9. Patil B. S. Wang Q. Hessel V. Lang J. Plasma N2-fixation: 1900–2014. *Catal. Today.* 2015;256:49–66. doi: 10.1016/j.cattod.2015.05.005. [CrossRef] [Google Scholar]
10. Wang G. Mitsos A. Marquardt W. Renewable production of ammonia and nitric acid. *AIChE J.* 2020;66(6):1–9. doi: 10.1002/aic.16947. [CrossRef] [Google Scholar]
11. Smil V. Global population and the nitrogen cycle. *Sci. Am.* 1997;277(1):76–81. doi: 10.1038/scientificamerican0797-76. [CrossRef] [Google Scholar]
12. Erisman J. W. Sutton M. A. Galloway J. Klimont Z. Winiwarter W. How a century of ammonia synthesis changed the world. *Nat. Geosci.* 2008;1(10):636–639. doi: 10.1038/ngeo325. [CrossRef] [Google Scholar]
13. Armijo J. Philibert C. Flexible production of green hydrogen and ammonia from variable solar and wind energy: Case study of Chile and Argentina. *Int. J. Hydrogen Energy.* 2020;45(3):1541–1558. doi: 10.1016/j.ijhydene.2019.11.028. [CrossRef] [Google Scholar]
14. Rouwenhorst K. H. R. Van Der Ham A. G. J. Mul G. Kersten S. R. A. Islanded ammonia power systems: Technology review & conceptual process design. *Renewable Sustainable Energy Rev.* 2019;114:109339. doi: 10.1016/j.rser.2019.109339. [CrossRef] [Google Scholar]
15. Smith C. Hill A. K. Torrente-Murciano L. Current and future role of Haber–Bosch ammonia in a carbon-free energy landscape. *Energy Environ. Sci.* 2020;13(2):331–344. doi: 10.1039/C9EE02873K. [CrossRef] [Google Scholar]
16. MacFarlane D. R. Cherepanov P. V. Choi J. Suryanto B. H. R. Hodgetts R. Y. Bakker J. M. Simonov A. N. A roadmap to the ammonia economy. *Joule.* 2020;4(6):1186–1205. doi: 10.1016/j.joule.2020.04.004. [CrossRef] [Google Scholar]
17. Bogaerts A. Neyts E. C. Plasma technology: an emerging technology for energy storage. *ACS Energy Lett.* 2018;3(4):1013–1027. doi: 10.1021/acsenergylett.8b00184. [CrossRef] [Google Scholar]
18. Nitrate Division, O. O. W. D. and Fixed Nitrogen Research Laboratory Department of Agriculture, *Report on the Fixation and Utilization of Nitrogen*, 1922 [Google Scholar]

19. Fridell E. Skoglundh M. Westerberg B. Johansson S. Smedler G. NO_x storage in barium-containing catalysts. *J. Catal.* 1999;183(2):196–209. doi: 10.1006/jcat.1999.2415. [CrossRef] [Google Scholar]

20. Farber E. From chemistry to philosophy: The way of Alwin Mittasch (1869–1953) *Chymia.* 1966;11:157–178. doi: 10.2307/27757266. [CrossRef] [Google Scholar]

21. Mittasch A. Frankenburg W. Early studies of multicomponent catalysts. *Adv. Catal.* 1950;2(C):81–104. doi: 10.1016/S0360-0564(08)60375-2. [CrossRef] [Google Scholar]

22. Prieto G. Schüth F. The Yin and Yang in the development of catalytic processes: Catalysis research and reaction engineering. *Angew. Chem., Int. Ed.* 2015;54(11):3222–3239. doi: 10.1002/anie.201409885. [PubMed] [CrossRef] [Google Scholar]

23. Rouwenhorst K. H. R., Krzywda P. M., Benes N. E., Mul G. and Lefferts L. (2020). Ammonia production technologies, in *Techno-Economic Challenges of Green Ammonia as Energy Vector*, ed. R. Bañares-Alcántara and A. Valera-Medina, Elsevier Science Publishing Co Inc., pp. 41–84. 10.1016/B978-0-12-820560-0.00004-7 [CrossRef] [Google Scholar]

24. Sánchez A. Martín M. Scale up and scale down issues of renewable ammonia plants: Towards modular design. *Sustainable Prod. Consumption.* 2018;16:176–192. doi: 10.1016/j.spc.2018.08.001. [CrossRef] [Google Scholar]

25. askIITians. (2020). Nitric Acid, Retrieved September 1, 2020, from https://www.askiitians.com/iit-jee-s-and-p-block-elements/nitric-acid/ [Google Scholar]

26. Birkeland K. On the oxidation of atmospheric nitrogen in electric arcs. *Trans. Faraday Soc.* 1906;2:98–116. [Google Scholar]

27. Eyde S. Oxidation of atmospheric nitrogen and development of resulting industries in Norway. *J. Ind. Eng. Chem.* 1912;4:771–774. [Google Scholar]

28. Rusanov V. D. Fridman A. A. Sholin G. V. The physics of a chemically active plasma with nonequilibrium vibrational excitation of molecules. *Phys.-Usp.* 1981;24(6):447–474. [Google Scholar]

29. Ammann P. R. Timmins R. S. Chemical reactions during rapid quenching of oxygen–nitrogen mixtures from very high temperatures. *AIChE J.* 1966;12:956–963. [Google Scholar]

30. Mehta P. Barboun P. Go D. B. Hicks J. C. Schneider W. F. Catalysis enabled by plasma activation of strong chemical bonds: A review. *ACS Energy Lett.* 2019;4(5):1115–1133. doi: 10.1021/acsenergylett.9b00263. [CrossRef] [Google Scholar]

31. Winter L. R. Chen J. G. N2 fixation by plasma-activated processes. *Joule.* 2020:1–16. doi: 10.1016/j.joule.2020.11.009. [CrossRef] [Google Scholar]

32. Liu H., *Ammonia Synthesis Catalysts: Innovation and Practice*, World Scientific, 2013 10.1142/8199 [CrossRef] [Google Scholar]

33. Jardali F. van Alphen S. Creel J. Eshtehardi H. A. Axelsson M. Ingels R. Bogaerts A. NO_x production in a rotating gliding arc plasma: potential avenue for sustainable nitrogen fixation. *Green Chem.* 2021;23(4):1748–1757. doi: 10.1039/D0GC03521A. [CrossRef] [Google Scholar]

34. Vervloessem E. Aghaei M. Jardali F. Hafezkhiabani N. Bogaerts A. Plasma-based N2 fixation into NO_x: Insights from modeling toward optimum yields and energy costs in a gliding arc plasmatron. *ACS Sustainable Chem. Eng.* 2020;8(26):9711–9720. doi: 10.1021/acssuschemeng.0c01815. [CrossRef] [Google Scholar]

35. Rapakoulias D. Cavadias S. Amouroux J. Processus catalytiques dans un réacteur à plasma hors d'équilibre II. Fixation de l'azote dans le système N2–O2. *Rev. Phys. Appl.* 1980;15(7):1261–1265. doi: 10.1051/rphysap:019800015070126100. [CrossRef] [Google Scholar]

36. Patil B. S. Cherkasov N. Lang J. Ibhadon A. O. Hessel V. Wang Q. Low temperature plasma-catalytic NO_x synthesis in a packed DBD reactor: Effect of support materials and supported active metal oxides. *Appl. Catal., B.* 2016;194:123–133. doi: 10.1016/j.apcatb.2016.04.055. [CrossRef] [Google Scholar]

37. Hessel V. Anastasopoulou A. Wang Q. Kolb G. Lang J. Energy, catalyst and reactor considerations for (near)-industrial plasma processing and learning for nitrogen-fixation reactions. *Catal. Today.* 2013;211:9–28. doi: 10.1016/j.cattod.2013.04.005. [CrossRef] [Google Scholar]

38. Michielsen I. Uytdenhouwen Y. Pype J. Michielsen B. Mertens J. Reiniers F. Bogaerts A. CO_2 dissociation in a packed bed DBD reactor: First steps towards a better understanding of plasma catalysis. *Chem. Eng. J.* 2017;326:477–488. doi: 10.1016/j.cej.2017.05.177. [CrossRef] [Google Scholar]

39. Gicquel A. Cavadias S. Amouroux J. Heterogeneous catalysis in low-pressure plasmas. *J. Phys. D: Appl. Phys.* 1986;19:2013–2042. [Google Scholar]

40. Mars P. van Krevelen D. W. Oxidations carried out by means of vanadium oxide catalysts. *Chem. Eng. Sci.* 1954;3:41–59. doi: 10.1016/S0009-2509(54)80005-4. [CrossRef] [Google Scholar]

41. Diekhöner L. Mortensen H. Baurichter A. N2 dissociative adsorption on Ru(0001): The role of energy loss. *J. Chem. Phys.* 2001;115(19):9028–9035. doi: 10.1063/1.1413746. [CrossRef] [Google Scholar]

42. Romm L. Katz G. Kosloff R. Asscher M. Dissociative chemisorption of N2 on Ru(001) enhanced by vibrational and kinetic energy: Molecular beam experiments and quantum mechanical calculations. *J. Phys. Chem. B.* 1997;101(12):2213–2217. doi: 10.1021/jp962599o. [CrossRef] [Google Scholar]

43. Pfnür H. E. Rettner C. T. Lee J. Madix R. J. Auerbach D. J. Dynamics of the activated dissociative chemisorption of N2 on W(110): A molecular beam study. *J. Chem. Phys.* 1986;85(12):7452–7466. doi: 10.1063/1.451334. [CrossRef] [Google Scholar]

44. Bogaerts A. Tu X. Whitehead J. C. Centi G. Lefferts L. Guaitella O. Carreon M. The 2020 plasma catalysis roadmap. *J. Phys. D: Appl. Phys.* 2020;53:1–51. doi: 10.1088/1361-6463/ab9048. [CrossRef] [Google Scholar]

45. Shi C. Yang X. F. Zhu A. M. Au C. T. Catalytic activities of tungsten nitride for NO dissociation and reduction with hydrogen. *Catal. Today.* 2004;93–95:819–826. doi: 10.1016/j.cattod.2004.06.102. [CrossRef] [Google Scholar]

46. Ma H. Schneider W. F. DFT and microkinetic comparison of Pt, Pd and Rh-catalyzed ammonia oxidation. *J. Catal.* 2020;383:322–330. doi: 10.1016/j.jcat.2020.01.029. [CrossRef] [Google Scholar]

47. Rouwenhorst K. H. R. Engelmann Y. Van't Veer K. Postma R. S. Bogaerts A. Lefferts L. Plasma-driven catalysis: Green ammonia synthesis with intermittent electricity. *Green Chem.* 2020;22(19):6258–6287. doi: 10.1039/D0GC02058C. [CrossRef] [Google Scholar]

48. Sun Q. Wang Z. Wang D. Hong Z. Zhou M. Li X. A review on the catalytic decomposition of NO to N2 and O2: Catalysts and processes. *Catal. Sci. Technol.* 2018;8(18):4563–4575. doi: 10.1039/c8cy01114a. [CrossRef] [Google Scholar]

49. Haneda M. Hamada H. Recent progress in catalytic NO decomposition. *Compt. Rend. Chim.* 2016;19(10):1254–1265. doi: 10.1016/j.crci.2015.07.016. [CrossRef] [Google Scholar]

50. Imanaka N. Masui T. Advances in direct NO_x decomposition catalysts. *Appl. Catal., A.* 2012;431–432:1–8. doi: 10.1016/j.apcata.2012.02.047. [CrossRef] [Google Scholar]

51. Taugbøl T., Andersen E. M., Grønn U. and Moen B. F., Rjukan – Notodden Industrial Heritage Site, 2015, retrieved from https://www.visitrjukan.com/en/content/download/6296/35783/file/Verdensarv_engelsk_industriarv_Nomination.pdf [Google Scholar]

52. Rehbein N. Cooray V. NO_x production in spark and corona discharges. *J. Electrostat.* 2001;51–52(1–4):333–339. doi: 10.1016/S0304-3886(01)00115-2. [CrossRef] [Google Scholar]

53. Pei X. Gidon D. Yang Y. J. Xiong Z. Graves D. B. Reducing energy cost of NO_x production in air plasmas. *Chem. Eng. J.* 2019;362:217–228. doi: 10.1016/j.cej.2019.01.011. [CrossRef] [Google Scholar]

54. Janda M. Martišovitš V. Hensel K. Machala Z. Generation of antimicrobial NO_x by atmospheric air transient spark discharge. *Plasma Chem. Plasma Proc.* 2016;36:767–781. doi: 10.1007/s11090-016-9694-5. [CrossRef] [Google Scholar]

55. Pavlovich M. J. Ono T. Galleher C. Curtis B. Clark D. S. Machala Z. Graves D. B. Air spark-like plasma source for antimicrobial NO_x generation. *J. Phys. D: Appl. Phys.* 2014;47(50):505202. doi: 10.1088/0022-3727/47/50/505202. [CrossRef] [Google Scholar]

56. Partridge W. S. Parlin R. B. Zwolinski B. J. Fixation of nitrogen in a crossed discharge. *Ind. Eng. Chem.* 1954;46(7):1468–1471. [Google Scholar]

57. Rahman M. Cooray V. NO_x generation in laser-produced plasma in air as a function of dissipated energy. *Opt. Laser Technol.* 2003;35(7):543–546. doi: 10.1016/S0030-3992(03)00077-X. [CrossRef] [Google Scholar]

58. Bian W. Shi J. Yin X. Nitrogen fixation into water by pulsed high-voltage discharge. *IEEE Trans. Plasma Sci.* 2009;37(1):211–218. doi: 10.1109/TPS.2008.2007585. [CrossRef] [Google Scholar]

59. Pei X. Gidon D. Graves D. B. Specific energy cost for nitrogen fixation as NO_xusing DC glow discharge in air. *J. Phys. D: Appl. Phys.* 2020;53:044002. doi: 10.1088/1361-6463/ab5095. [CrossRef] [Google Scholar]

60. Coudert J. F., Baronnet J. M., Rakowitz J. and Fauchais P., Synthesis of nitrogen oxides in a plasma produced by a jet arc generator, in *Symp. Int. Chim. Plasmas*, 1977 [Google Scholar]

61. Patil B. S. Peeters F. J. J. van Rooij G. J. Medrano J. A. Gallucci F. Lang J. Hessel V. Plasma assisted nitrogen oxide production from air: Using pulsed powered gliding arc reactor for a containerized plant. *AIChE J.* 2018;64(2):526–537. doi: 10.1002/aic.15922. [CrossRef] [Google Scholar]

62. Wang W. Patil B. Heijkers S. Hessel V. Bogaerts A. Nitrogen fixation by gliding arc plasma: Better insight by chemical kinetics modelling. *ChemSusChem.* 2017;10(10):2145–2157. doi: 10.1002/cssc.201700095. [PubMed] [CrossRef] [Google Scholar]

63. Kim T. Song S. Kim J. Iwasaki R. Formation of NO_x from air and N2/O2 mixtures using a nonthermal microwave plasma system. *Jpn. J. Appl. Phys.* 2010;49:126201. doi: 10.1143/JJAP.49.126201. [CrossRef] [Google Scholar]

64. Mutel B. Dessaux O. Goudmand P. Energy cost improvement of the nitrogen oxides synthesis in a low pressure plasma. *Rev. Phys. Appl.* 1984;19(6):461–464. doi: 10.1051/rphysap:01984001906046100. [CrossRef] [Google Scholar]

65. Asisov R. I. Givotov V. K. Rusanov V. D. Fridman A. High energy chemistry. *Sov. Phys.* 1980;14:366. [Google Scholar]

66. Peng P. Chen P. Addy M. Cheng Y. Zhang Y. Anderson E. Ruan R. *In situ* plasma-assisted atmospheric nitrogen fixation using water and spray-type jet plasma. *Chem. Commun.* 2018;54(23):2886–2889. doi: 10.1039/c8cc00697k. [PubMed] [CrossRef] [Google Scholar]

67. Gorbanev Y. Vervloessem E. Nikiforov A. Bogaerts A. Nitrogen fixation with water vapor by non-equilibrium plasma: Towards sustainable ammonia production. *ACS Sustainable Chem. Eng.* 2020;8(7):2996–3004. doi: 10.1021/acssuschemeng.9b07849. [CrossRef] [Google Scholar]

68. Toth J. R. Abuyazid N. H. Lacks D. J. Renner J. N. Sankaran R. M. A plasma-water droplet reactor for process-intensified continuous nitrogen fixation at atmospheric pressure. *ACS Sustainable Chem. Eng.* 2020;8(39):14845–14854. doi: 10.1021/acssuschemeng.0c04432. [CrossRef] [Google Scholar]

69. Peng P. Schiappacasse C. Zhou N. Addy M. Cheng Y. Zhang Y. Anderson E. Chen D. Wang Y. Liu Y. Chen P. Ruan R. Plasma *in situ* gas–liquid nitrogen fixation using concentrated high-intensity electric field. *J. Phys. D: Appl. Phys.* 2019;52(49):494001. doi: 10.1088/1361-6463/ab3ea6. [CrossRef] [Google Scholar]

70. Kubota Y. Koga K. Ohno M. Hara T. Synthesis of ammonia through direct chemical reactions between an atmospheric nitrogen plasma jet and a liquid. *Plasma Fus. Res.* 2010;5:042. doi: 10.1585/pfr.5.042. [CrossRef] [Google Scholar]

71. Kumari S. Pishgar S. Schwarting M. E. Paxton W. F. Spurgeon J. M. Synergistic plasma-assisted electrochemical reduction of nitrogen to ammonia. *Chem. Commun.* 2018;54(95):13347–13350. doi: 10.1039/c8cc07869f. [PubMed] [CrossRef] [Google Scholar]

72. Hawtof R. Ghosh S. Guarr E. Xu C. Sankaran R. M. Renner J. N. Catalyst-free, highly selective synthesis of ammonia from nitrogen and water by a plasma electrolytic system. *Asian J. Chem.* 2019;31(2):1–10. doi: 10.1126/sciadv.aat5778. [PMC free article] [PubMed] [CrossRef] [Google Scholar]

73. Haruyama T. Namise T. Shimoshimizu N. Uemura S. Takatsuji Y. Hino M. Kohno M. Non-catalyzed one-step synthesis of ammonia from atmospheric air and water. *Green Chem.* 2016;18(16):4536–4541. doi: 10.1039/c6gc01560c. [CrossRef] [Google Scholar]

74. Sakakura T. Uemura S. Hino M. Kiyomatsu S. Takatsuji Y. Yamasaki R. Haruyama T. Excitation of H2O at the plasma/water interface by UV irradiation for the elevation of ammonia production. *Green Chem.* 2018;20(3):627–633. doi: 10.1039/c7gc03007j. [CrossRef] [Google Scholar]

75. Sakakura T. Murakami N. Takatsuji Y. Morimoto M. Haruyama T. Contribution of discharge excited atomic N, N2*, and N2+ to a plasma/liquid interfacial reaction as suggested by quantitative analysis. *ChemPhysChem.* 2019;20(11):1467–1474. doi: 10.1002/cphc.201900212. [PubMed] [CrossRef] [Google Scholar]

76. Sakakura T. Murakami N. Takatsuji Y. Haruyama T. Nitrogen fixation in a plasma/liquid interfacial reaction and its switching between reduction and oxidation. *J. Phys. Chem. C.* 2020;124(17):9401–9408. doi: 10.1021/acs.jpcc.0c02392. [CrossRef] [Google Scholar]

77. Polak L. S., Ovsiannikov A. A., Slovetsky D. I. and Vurzel F. B., Theoretical and applied plasma chemistry, *Nauka (Science)*, 1975 [Google Scholar]

78. Ivanov A. A. Plasma physics. *Sov. Phys.* 1975;1:147. [Google Scholar]

79. Krop J. Krop E. Pollo I. Calculated amounts of nitric oxide in a nitrogen–oxygen plasma jet. *Chem. Plazmy.* 1979:242–249. [Google Scholar]

80. Hao X. Mattson A. M. Edelblute C. M. Malik M. A. Heller L. C. Kolb J. F. Nitric oxide generation with an air operated non-thermal plasma jet and associated microbial inactivation mechanisms. *Plasma Proc. Polym.* 2014;11(11):1044–1056. doi: 10.1002/ppap.201300187. [CrossRef] [Google Scholar]

81. Korolev Y. D. Frants O. B. Landl N. V. Suslov A. I. Low-current plasmatron as a source of nitrogen oxide molecules. *IEEE Trans. Plasma Sci.* 2012;40(11):2837–2842. doi: 10.1109/TPS.2012.2201755. [CrossRef] [Google Scholar]

82. Ingels R., *Energy efficient process for producing nitrogen oxide*, Norway, 2012 [Google Scholar]

83. Patel H. Sharma R. K. Kyriakou V. Pandiyan A. Welzel S. Tsampas M. N. Plasma-activated electrolysis for cogeneration of nitric oxide and hydrogen from water and nitrogen. *ACS Energy Lett.* 2019;4(9):2091–2095. doi: 10.1021/acsenergylett.9b01517. [CrossRef] [Google Scholar]
rapid-communication

84. Pipa A. V. Bindemann T. Foest R. Kindel E. Röpcke J. Weltmann K.-D. Absolute production rate measurements of nitric oxide by an atmospheric pressure plasma jet (APPJ) *J. Phys. D: Appl. Phys.* 2008;41:194011. doi: 10.1088/0022-3727/41/19/194011. [CrossRef] [Google Scholar]

85. Sun Q. Zhu A. Yang X. Niu J. Xu Y. Formation of NO_x from N2 and O2 in catalyst-pellet filled dielectric barrier discharges at atmospheric pressure. *Chem. Commun.* 2003:1418–1419. doi: 10.1039/B303046F. [PubMed] [CrossRef] [Google Scholar]

86. Abdelaziz A. A. Kim H.-H. Temperature-dependent behavior of nitrogen fixation in nanopulsed dielectric barrier discharge operated at different humidity levels and oxygen contents. *J. Phys. D: Appl. Phys.* 2020;53:114001. doi: 10.1088/1361-6463/ab5c78. [CrossRef] [Google Scholar]

87. Heijkers S. Snoeckx R. Kozák T. Silva T. Godfroid T. Britun N. Bogaerts A. CO_2 conversion in a microwave plasma reactor in the presence of N_2: Elucidating the role of vibrational levels. *J. Phys. Chem. C.* 2015;119(23):12815–12828. doi: 10.1021/acs.jpcc.5b01466. [CrossRef] [Google Scholar]

88. Berthelot A. Bogaerts A. Modeling of CO_2 splitting in a microwave plasma: How to improve the conversion and energy efficiency. *J. Phys. Chem. C.* 2017;121(15):8236–8251. doi: 10.1021/acs.jpcc.6b12840. [CrossRef] [Google Scholar]

89. Czernichowski A. Gliding arc. Applications to engineering and environment control. *Pure Appl. Chem.* 1994;66(6):1301–1310. doi: 10.1351/pac199466061301. [CrossRef] [Google Scholar]

90. Ramakers M. Trenchev G. Heijkers S. Wang W. Bogaerts A. Gliding arc plasmatron: Providing an alternative method for carbon dioxide conversion. *ChemSusChem.* 2017;10(12):2642–2652. doi: 10.1002/cssc.201700589. [PubMed] [CrossRef] [Google Scholar]

91. Patil B. S. Rovira Palau J. Hessel V. Lang J. Wang Q. Plasma nitrogen oxides synthesis in a milli-scale gliding arc reactor: Investigating the electrical and process parameters. *Plasma Chem. Plasma Proc.* 2016;36(1):241–257. doi: 10.1007/s11090-015-9671-4. [CrossRef] [Google Scholar]

92. Wang Y. DeSilva A. W. Goldenbaum G. C. Dickerson R. R. Nitric oxide production by simulated lightning: Dependence on current, energy, and pressure. *J. Geophys. Res. Atmos.* 1998;103(D15):19149–19159. doi: 10.1029/98JD01356. [CrossRef] [Google Scholar]

93. Adamovich I., Rich W., Chernukho P. and Zhdanok S., Analysis of the power budget and stability of high-pressure nonequilibrium air plasmas, in *31st Plasmadynamics and Laser Conference*, Denver (CO), 2000 [Google Scholar]

94. Namihira T. Katsuki S. Hackam R. Akiyama H. Okamoto K. Production of nitric oxide using a pulsed arc discharge. *IEEE Trans. Plasma Sci.* 2002;30(5):1993–1998. doi: 10.1109/TPS.2002.807502. [CrossRef] [Google Scholar]

95. Namihira T. Sakai S. Matsuda M. Wang D. Kiyan T. Akiyama H. Toda K. Temperature and nitric oxide generation in a pulsed arc discharge plasma. *Plasma Sci. Technol.* 2007;9(6):747–751. doi: 10.1088/1009-0630/9/6/26. [CrossRef] [Google Scholar]

96. Cleiren E. Heijkers S. Ramakers M. Bogaerts A. Dry reforming of methane in a gliding arc plasmatron: Towards a better understanding of the plasma chemistry. *ChemSusChem.* 2017;10(20):4025–4036. doi: 10.1002/cssc.201701274. [PubMed] [CrossRef] [Google Scholar]

97. Janda M. Martišovitš V. Hensel K. Dvonč L. Machala Z. Measurement of the electron density in transient spark discharge. *Plasma Sources Sci. Technol.* 2014;23(6):065016. doi: 10.1088/0963-0252/23/6/065016. [CrossRef] [Google Scholar]

98. Janda M. Hoder T. Sarani A. Brandenburg R. Machala Z. Cross-correlation spectroscopy study of the transient spark discharge in atmospheric pressure air. *Plasma Sources Sci. Technol.* 2017;26:055010. doi: 10.1088/1361-6595/aa642a. [CrossRef] [Google Scholar]

99. Bogaerts A. Centi G. Plasma technology for CO2 conversion: A personal perspective on prospects and gaps. *Front. Energy Res.* 2020;8:1–23. doi: 10.3389/fenrg.2020.00111. [CrossRef] [Google Scholar]

100. Bruggeman P. J. Iza F. Brandenburg R. Foundations of atmospheric pressure non-equilibrium plasmas. *Plasma Sources Sci. Technol.* 2017;26:123002. doi: 10.1088/1361-6595/aa97af. [CrossRef] [Google Scholar]

101. Van Alphen S. Vermeiren V. Butterworth T. van den Bekerom D. C. M. Van Rooij G. J. Bogaerts A. Power pulsing to maximize vibrational excitation efficiency in N2 microwave plasma: A combined experimental and computational study. *J. Phys. Chem. C.* 2019;124(3):1765–1779. doi: 10.1021/acs.jpcc.9b06053. [CrossRef] [Google Scholar]

102. Anastasopoulou A. Keijzer R. Butala S. Lang J. Van Rooij G. Hessel V. Eco-efficiency analysis of plasma-assisted nitrogen fixation. *J. Phys. D: Appl. Phys.* 2020;53:234001. doi: 10.1088/1361-6463/ab71a8. [CrossRef] [Google Scholar]

103. Morgan E. R. Manwell J. F. McGowan J. G. Sustainable ammonia production from U.S. offshore wind farms: A techno-economic review. *ACS Sustainable Chem. Eng.* 2017;5(11):9554–9567. doi: 10.1021/acssuschemeng.7b02070. [CrossRef] [Google Scholar]

104. Peters M. S., Timmerhaus K. D. and West R. E., *Plant Design and Economics for Chemical Engineers*, Mac Graw and Hill, 2003 [Google Scholar]

105. van Rooij G. J. Akse H. N. Bongers W. A. van de Sanden M. C. M. Plasma for electrification of chemical industry: A case study on CO_2 reduction. *Plasma Phys. Controlled Fus.* 2018;60:014019. doi: 10.1088/1361-6587/aa8f7d. [CrossRef] [Google Scholar]

106. Kirschner M. J., Alekseev A., Dowy S., Grahl M., Jansson L., Keil P. and Windmeier C., Oxygen, in *Ullmann's Encyclopedia of Industrial Chemistry*, Wiley-VCH Verlag GmbH & Co. KGaA, 2017 10.1002/14356007.a18_329.pub2 [CrossRef] [Google Scholar]

107. Appl M., in *Ammonia: Principles and Industrial Practice*, 1st edn, ed. M. Appl, Wiley-VCH Verlag GmbH, Weinheim (Germany), 1999 10.1002/9783527613885 [CrossRef] [Google Scholar]

108. Nayak-Luke R. M. Bañares-Alcántara R. Techno-economic viability of islanded green ammonia as a carbon-free energy vector and as a substitute for conventional production. *Energy Environ. Sci.* 2020;13(9):2957–2966. doi: 10.1039/d0ee01707h. [CrossRef] [Google Scholar]

109. Anastasopoulou A. Butala S. Patil B. Suberu J. Fregene M. Lang J. Hessel V. Techno-economic feasibility study of renewable power systems for a small-scale plasma-assisted nitric acid plant in Africa. *Processes.* 2016;4(4):54. doi: 10.3390/pr4040054. [CrossRef] [Google Scholar]

110. Lin B. Wiesne T. Malmali M. Performance of a small-scale Haber process: A techno-economic analysis. *ACS Sustainable Chem. Eng.* 2020;8(41):15517–15531. doi: 10.1021/acssuschemeng.0c04313. [CrossRef] [Google Scholar]

111. Van Alphen S. Jardali F. Creel J. Trenchev G. Snyders R. Bogaerts A. Sustainable gas conversion by gliding arc plasmas: A new modelling approach for reactor design improvement. *Sustainable Energy Fuels.* 2021;5(6):1786–1800. doi: 10.1039/D0SE01782E. [CrossRef] [Google Scholar]

112. Vermeiren V. Bogaerts A. Plasma-based CO2 conversion: To quench or not to quench? *J. Phys. Chem. C.* 2020;124(34):18401–18415. doi: 10.1021/acs.jpcc.0c04257. [CrossRef] [Google Scholar]

113. Brandenburg R. Bogaerts A. Bongers W. Fridman A. Fridman G. Locke B. R. Ostrikov K. K. White paper on the future of plasma science in environment, for gas conversion and agriculture. *Plasma Proc. Polym.* 2018:1–18. doi: 10.1002/ppap.201700238. [CrossRef] [Google Scholar]